

Electronic Supporting Information

for

Boron and nitrogen co-doped single-layered graphene quantum dots: a high-affinity platform for visualizing the dynamic invasions of HIV DNA into living cells through fluorescence resonance energy transfer

Rong Sheng Li,^{a, d} Binfang Yuan,^{b, c, d} Jia Hui Liu,^a Meng Li Liu,^b Peng Fei Gao,^a Yuan Fang Li,^b Ming Li,^b and Cheng Zhi Huang^{a, b, *}

^a Key Laboratory of Luminescent and Real-Time Analytical Chemistry (Southwest University), Ministry of Education, College of Pharmaceutical Sciences, Southwest University, Chongqing 400715, China. E-mail: chengzhi@swu.edu.cn; Tel: (+86) 23 68254059, Fax: (+86) 23 68367257. ^b College of Chemistry and Chemical Engineering, Southwest University, Chongqing 400715, China. ^c Department of Chemistry and Chemical Engineering, Yangtze Normal University, Chongqing 408100, PR China. ^d These authors contributed equally to this work.

Materials and apparatus

Oligonucleotide sequence used are listed below (mismatch underlined):

(1) BHQ2 dye-labeled ssDNA (P):

5'-BHQ2- 50-AGT CAG TGT GGA AAA TCT CTA GC-3'

(2) Complementary target HIV DNA (T1):

5'-GCT AGA GAT TTT CCA CAC TGA CT-3'

(3) Single-base mismatched target (T2):

5'-GCT AGA GAT TTT CTA CAC TGA CT-3'

(4) Random target (T3):

5'-TAT TCG TGA TG TCT AAT TGT CA-3'

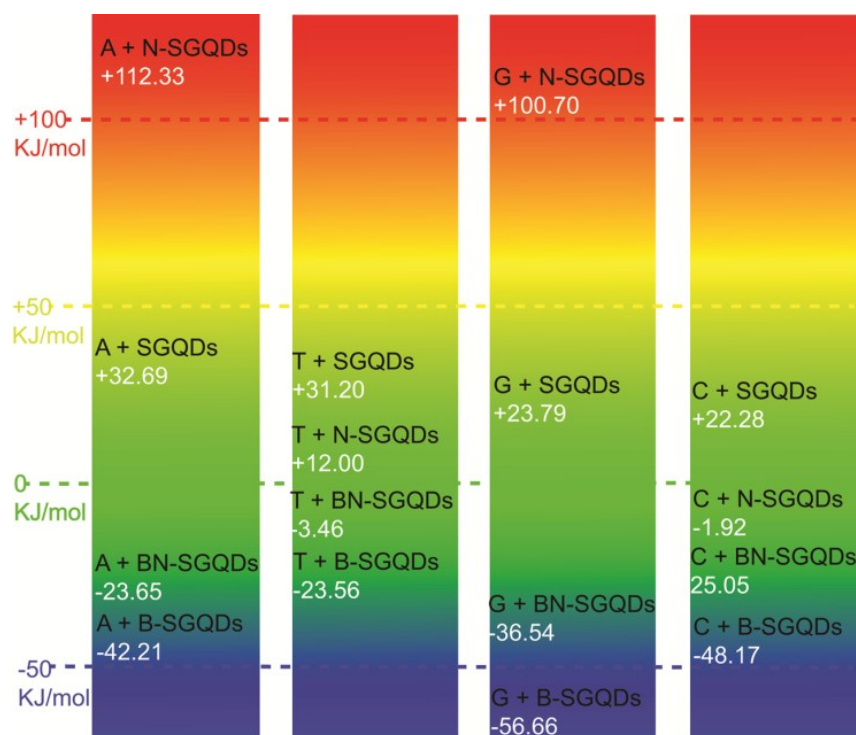


Figure S1. The changes of Gibbs free energy when nucleobases, A, T, G, and C, absorb on SGQDs, BN-SGQDs, N-SGQDs, and B-SGQDs. A: adenine; T: thymine; C: cytosine; G: guanine. Nitrogen doped single layer graphene quantum dots: N-SGQDs. Boron doped single layer graphene quantum dots: B-SGQDs.

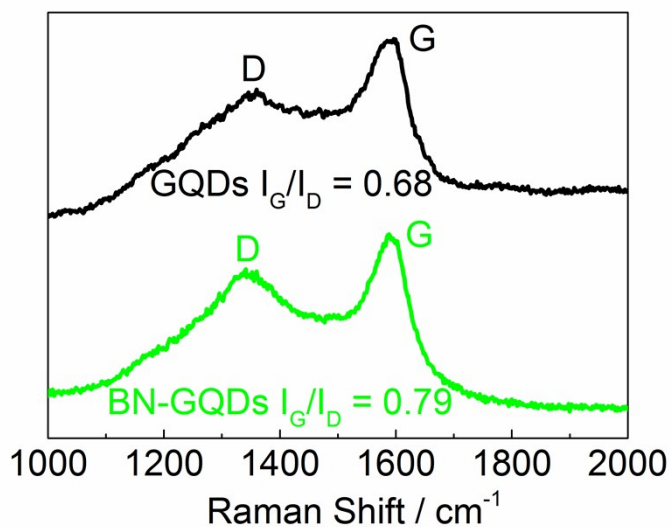


Figure S2. Raman spectra for SGQDs and BN-SGQDs.

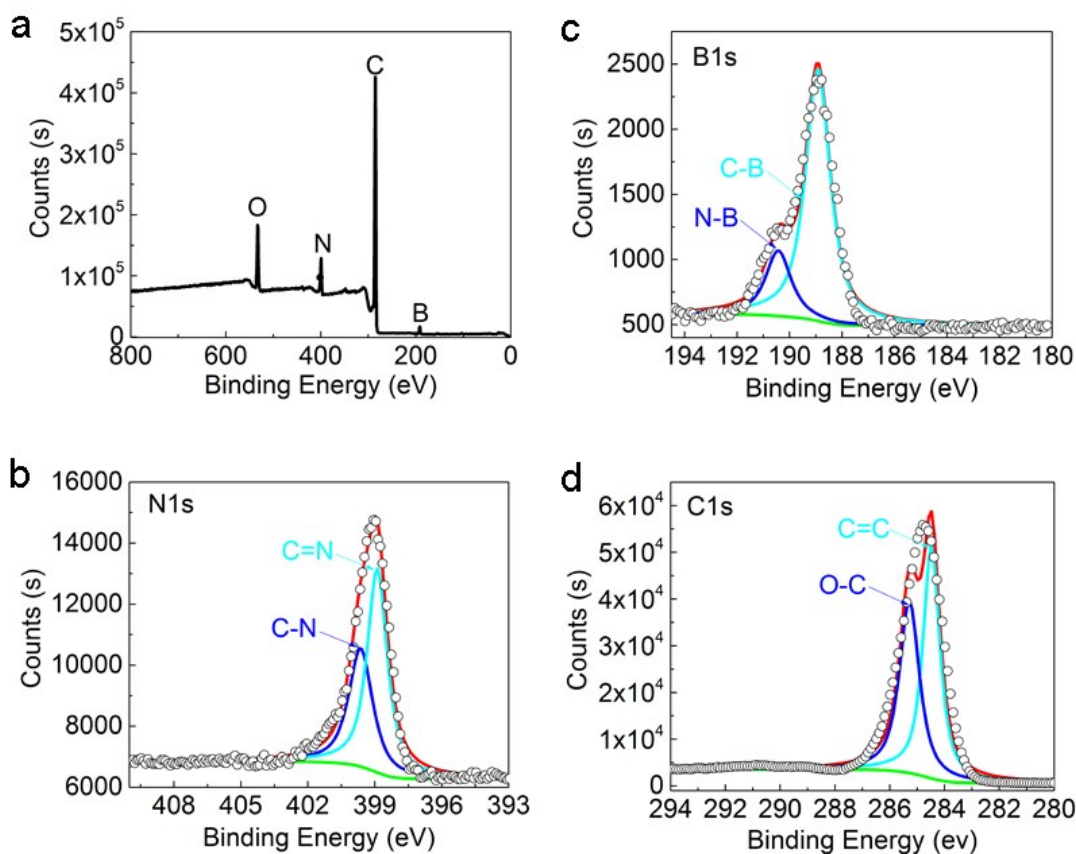


Figure S3. XPS survey of BN-SGQDs. (a) The wide scan spectra of BN-SGQDs. (b) The high-resolution N 1s XPS spectrum of BN-SGQDs. (c) The high-resolution B 1s XPS spectrum of BN-SGQDs. (d) The high-resolution C 1s XPS spectrum of BN-SGQDs.

Date notes:

The nature of doping is identified by Raman spectra and X-ray photoelectron spectroscopy (XPS) with peak deconvolution. The N and B concentrations for BN-SGQDs are 7.8 and 5.9 at.%, respectively (Figure S3a). Figure S2 shows the room temperature Raman spectra for graphene oxide (GO) and BN-SGQDs at 514.3 nm excitation. The I_G/I_D is a known parameter in evaluating the degree of graphitization.¹ The G band at 1580 cm^{-1} originates from the E_{2g} symmetry in-plane stretching mode, which is observed in an ordered graphene structure, and the D band at 1352 cm^{-1} originates from in-plane vibration resulting from structure imperfection.² The G-band of BN-SGQDs shows a decrease in intensity,

suggesting that the presence of B and N heteroatoms in the target is bringing about a noticeable change in the ordering degree of the hexagonal lattice. The decomposed peaks of N1s fitted by Gaussian curves are 398.8 and 399.7 eV (Figure S3b), which are assigned as pyridine-like nitrogen bonding with neighboring atom vacancy and graphite-like nitrogen bonding, respectively.² B1s spectra show that they are formed by different components (Figure S3c). The decomposed peaks of 188.9 and 190.4 eV are assigned as BC₃ and BN, respectively.^{1,3} These results suggest that boron and nitrogen have successfully doped in the graphene quantum dots.

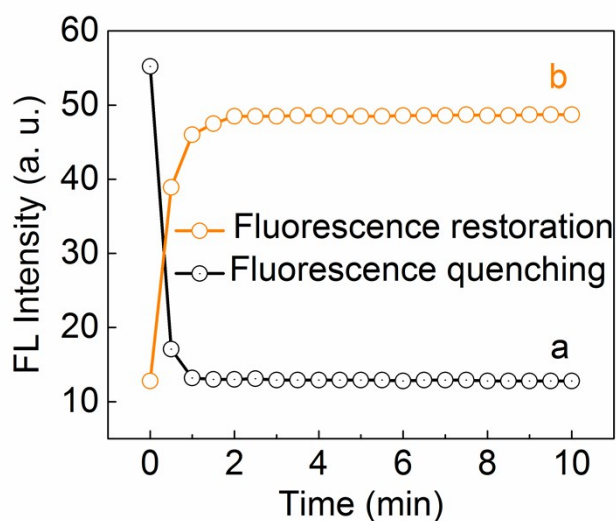


Figure S4. The detection time of BN-SGQDs as a DNA sensing platform. (a) Fluorescence quenching of BN-SGQDs ($50 \mu\text{g mL}^{-1}$) by P (100 nM) as a function of time. (b) Fluorescence restoration of BN-SGQDs + P complex by HIV DNA T1 (100 nM) as a function of time.

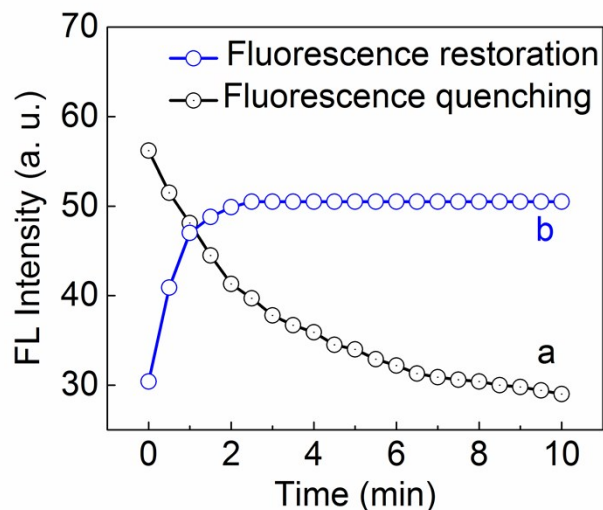


Figure S5. The detection time of undoped SGQDs as a DNA sensing platform. (a) Fluorescence quenching of SGQDs ($480 \mu\text{g mL}^{-1}$) by P (960 nM) as a function of time. (b) Fluorescence restoration of BN-SGQDs + P complex by HIV DNA T1 (960 nM) as a function of time.

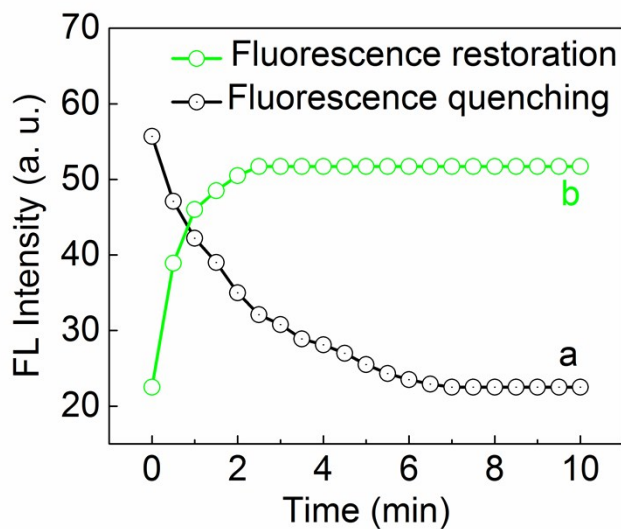


Figure S6. The detection time of nitrogen doped SGQDs (N-SGQDs) as a DNA sensing platform. (a) Fluorescence quenching of N-SGQDs ($213 \mu\text{g mL}^{-1}$) by P (426 nM) as a function of time. (b) Fluorescence restoration of N-SGQDs + P complex by HIV DNA T1 (426 nM) as a function of time.

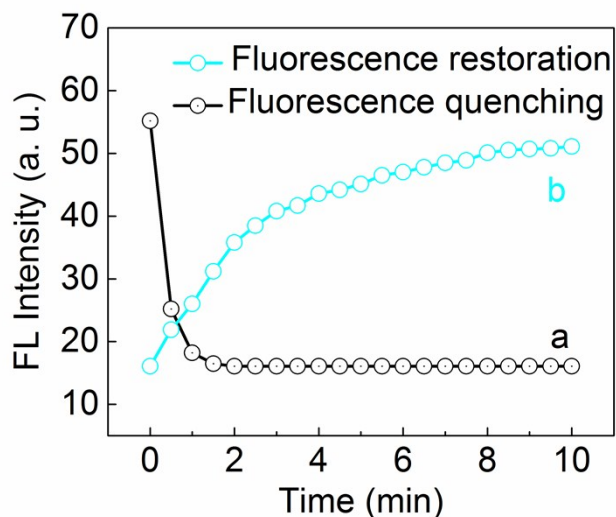


Figure S7. The detection time of boron doped SGQDs (B-SGQDs) as a DNA sensing platform. (a) Fluorescence quenching of B-SGQDs ($289 \mu\text{g mL}^{-1}$) by P (578 nM) as a function of time. (b) Fluorescence restoration of B-SGQDs + P complex by HIV DNA T1 (578 nM) as a function of time.



Figure S8. Selectivity of other SGQDs undoped or doped with N or B. (a) Selectivity of SGQDs + P complex by using complementary target DNA (T1), single-base mismatch DNA (T2), and random DNA (T3). (b) Selectivity of N-SGQDs + P complex by using complementary target DNA (T1), single-base mismatch DNA (T2), and random DNA (T3). (c) Selectivity of B-SGQDs + P complex by using complementary target DNA (T1), single-base mismatch DNA (T2), and random DNA (T3). Error bars were obtained from three parallel experiments.

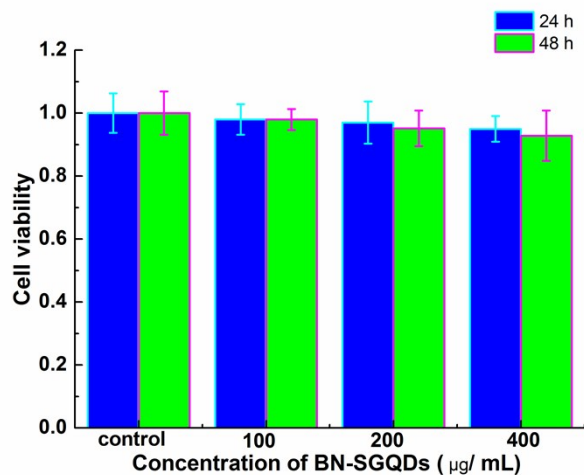


Figure S9. Cell viability of HeLa cells with Cell Counting Kit-8. The viability of HeLa cells was detected by incubating cells with HeLa at different concentrations and for different time. The results indicate the good biocompatibility of HeLa.

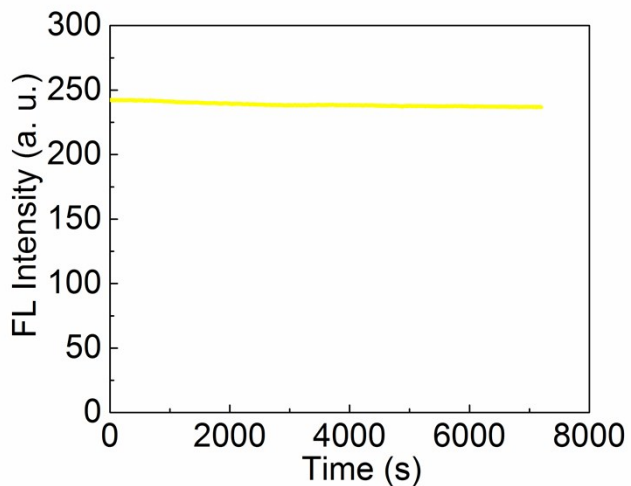


Figure S10. Photostability of BN-SGQDs aqueous solution under continuous irradiation at 400 nm.

Table S1. Comparison of different carbon nanoplatfoms of DNA sensing.

Type	Sensitivity	Detection time	DNA adsorption & photoluminescence	size	Reference
SWNT-based DNA detection	4.0 nM	Slow (several hour)	No	nanowire > 200 nm	4
GO-based DNA detection (premixing)	10.0 nM	Slow (0.5h)	No	Nanosheet > 200 nm	5
GO-based DNA detection (postmixing)	100 pM	Fast (\approx 1 min)	No	Nanosheet > 200 nm	6
CNPs-based DNA detection	33.0 nM	Slow (1h)	No	Sphere >25 nm	7
cCQDs-based DNA detection	17.4 nM	Slow (70 min)	No	Sphere 24.7 nm	8
BN-SGQDs-based DNA detection	0.5 nM	Fast (4 min)	Yes	Nanosheet 8.1 nm	This work

References

1. B. Dai, K. Chen, Y. Wang, L. Kang and M. Zhu, *ACS Catal.*, 2015, **5**, 2541-2547.
2. R. Yuge, S. Bandow, M. Yudasaka, K. Toyama, S. Iijima and T. Manako, *Carbon*, 2017, **111**, 675-680.
3. Y. Zheng, Y. Jiao, L. Ge, M. Jaroniec and S. Z. Qiao, *Angew. Chem.*, 2013, **125**, 3192-3198.
4. R. Yang, J. Jin, Y. Chen, N. Shao, H. Kang, Z. Xiao, Z. Tang, Y. Wu, Z. Zhu and W. Tan, *J. Am. Chem. Soc.*, 2008, **130**, 8351-8358.
5. C.-H. Lu, H.-H. Yang, C.-L. Zhu, X. Chen and G.-N. Chen, *Angew. Chem.*, 2009, **121**, 4879-4881.
6. S. He, B. Song, D. Li, C. Zhu, W. Qi, Y. Wen, L. Wang, S. Song, H. Fang and C. Fan, *Adv. Funct. Mater.*, 2010, **20**, 453-459.
7. H. Li, Y. Zhang, L. Wang, J. Tian and X. Sun, *Chem. Commun.*, 2011, **47**, 961-963.
8. A. H. Loo, Z. Sofer, D. Bouša, P. Ulbrich, A. Bonanni and M. Pumera, *ACS Appl. Mater. Inter.*, 2016, **8**, 1951-1957.